SEMARAK ILMU PUBLISHING

Journal of Advanced Research in Fluid Mechanics and Thermal Sciences

Journal homepage:
https://semarakilmu.com.my/journals/index.php/fluid_mechanics_thermal_sciences/index
ISSN: 2289-7879

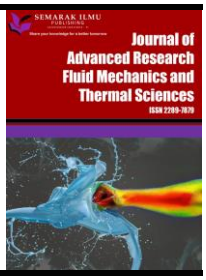

Application of Keller-Box Method to the Heat and Mass Transfer Analysis of Magnetohydrodynamic Flow of Micropolar Fluid between Porous Parallel Walls of Different Permeability

Ashwini Bhat[1,*], Param Tangsali[1], Nagaraj Nagesh Katagi[1]

[1] Department of Mathematics, Manipal Institute of Technology, Manipal Academy of Higher Education, Manipal, Karnataka, India

ARTICLE INFO

Article history:
Received 15 August 2022
Received in revised form 26 December 2022
Accepted 4 January 2023
Available online 25 January 2023

Keywords:
Micropolar fluid; channel flow; permeability; Keller-Box method; heat and mass transfer

ABSTRACT

The present work seeks to investigate the problem of stable laminar micropolar fluid flow through porous walls of varying permeability. Furthermore, the effect of an external magnetic field is investigated. The resulting solution is extended to analyse the nonlinear differential equation of heat and mass transfer in the flow situation. The velocity and microrotation at the channel's entrance are assumed to be those of Poiseuille flow. Using appropriate transformations, the governing nonlinear equations are transformed to a system of ordinary differential equations, which are then solved using a novel numerical technique based on a finite difference scheme termed the Keller-box method. The results show that the smooth and straightforward Keller-box method is an appropriate method for estimating solutions of complex governing equations since it is simple to implement. Graphs and tables are used to explain the effect of significant parameters such as the suction Reynolds number, micro rotation/angular velocity parameters, and Peclet number on the stream function, temperature distribution, and concentration properties of the fluid. The effect of wall permeability on longitudinal velocity and microrotation has been investigated. The couple stress and skin friction on the walls have also been calculated. The effect of variation in Reynolds number is showing the importance of inertial forces in comparison with viscous forces. The velocity boundary layer is observed to decrease when there is an increase in Reynolds number. Furthermore, the accuracy and convergence of the obtained solutions show that the Keller-box method is applicable to various nonlinear physical problems, even those with significant non-linearity.

1. Introduction

Exploration exercises aimed at investigating fluid material science at the micro and nano scales have grown in popularity in recent years. The fluid flows in channels using Navier-Stokes equations have been thoroughly studied in the literature [1-8]. Because the Navier-Stokes equations do not account for molecular spin, they cannot explain fluid flow characteristics on a large scale, Eringen [9,10] established the theory of micro continuum, which explains the micropolar theory. This theory

* *Corresponding author.*
E-mail address: ashwini.bhat@manipal.edu

https://doi.org/10.37934/arfmts.102.2.186195

provided a mathematical framework for investigating the spinning effects in micropolar fluid motion. Because of the spinning micro ingredients, the micropolar fluid is extremely useful in modern engineering and technology. To understand theory behind the micropolar fluid flow and applications one can refer papers by Ariman *et al.,* [11,12] and Lukaazewicz [13].

The flow of micropolar fluid between porous channel were studied by Sastry *et al.,* [14]. They obtained the solution using numerical method followed by quasilinearisation. To better understand the behavior of micropolar fluids different authors have analyzed the flow situations using various semi-analytical and numerical techniques under different physical conditions [15-17]. Two-dimensional micropolar fluid flow in a porous channel with high mass transfer was studied by Kelson *et al.,* [18]. The governing equations were solved for huge mass transfer using semi-analytical perturbation technique. Later, the micropolar fluid flow driven by suction and injection on the channel walls is analyzed for high mass transfer using Optimal Homotopy Asymptotic Method [19]. The results were also validated with numerical solutions. It is well known fact that the presence of external magnetic force in any fluid flow situation alters the flow and have consequential effects on the flow parameters. The literature has witnessed a great amount of work on the analysis of micropolar fluid flow in fact in different geometries such as vertical plates, stretching sheets, tubes, disks and many more. The enormous applications of micropolar fluid flow in the existence of external magnetic force attracts research in this regard.

Thus, in the present study, our focus is to investigate the effect of suction and external magnetic force on the electrically conducting laminar flow of micropolar fluid in a channel with porous walls of varying permeability. The research is also extended to understand the heat and mass transfer processes in the current flow situation. We consider [9] Eringen's governing equations for the flow structure and model the problem with appropriate boundary conditions at the porous walls. The non-linear problem governing velocity and micro-rotation is solved by using finite difference box scheme also called Keller box method. The numerical outcomes are represented in relevant graphs and tables. The Keller-box method [20,21] is proven to be an efficient numerical procedure to solve highly non-linear governing equations. An extensive amount of explanation about the validation and application of this method can be extracted from the book [22].

2. Mathematical Formulation of the Problem

Consider the axi-symmetric laminar steady incompressible flow of an electrically conducting micropolar fluid between porous parallel walls of different permeability. Let the channel width be $2l$, with x and y axes chosen along and perpendicular to the porous walls. The fluid velocities along these axes are supposed to be u_x and u_y respectively. Let u_y be v_1 at the lower wall $y = -l$ while at the upper wall $y = l$, $u_y = v_2$. Without affecting the validity of the problem in general, we consider a particular case with $|v_2| \geq |v_1|$.

Assuming a stationary magnetic field B_0 in the transverse direction, which is perpendicular to the velocity field lying in the XY-plane. We neglect the induced magnetic field when compared to imposed field. It is also assumed that there is no applied electric field, i.e., $E = 0$. Also, assuming the absence of body couple, the linearized form of electromagnetic body force can be written as $-\sigma_e {B_0}^2 u_x$, where σ_e is electrical conductivity of fluid. The geometry of the flow situation can be visualized in Figure 1.

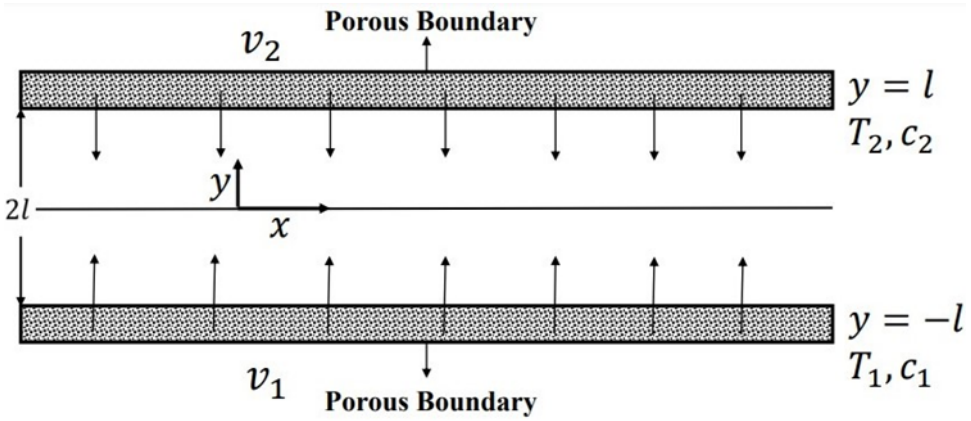

Fig. 1. Visualisation of the geometry in XY −plane

We use the governing theory proposed by Eringen for micropolar fluids, the equations for the magnetohydrodynamic laminar viscous incompressible steady flow of micropolar fluid are

$$\frac{\partial u_x}{\partial x} + \frac{1}{l}\frac{\partial u_y}{\partial \xi} = 0 \tag{1}$$

$$\rho\left(u_x\frac{\partial u_x}{\partial x} + \frac{u_y}{l}\frac{\partial u_x}{\partial \xi}\right) = (\mu + \kappa)\left(\frac{\partial^2 u_x}{\partial x^2} + \frac{1}{l^2}\frac{\partial^2 u_x}{\partial \xi^2}\right) + \frac{\kappa}{l}\frac{\partial v_m}{\partial \xi} - \frac{\partial p}{\partial x} - \sigma_e {B_0}^2 u_x \tag{2}$$

$$\rho\left(u_x\frac{\partial u_y}{\partial x} + \frac{u_y}{l}\frac{\partial u_y}{\partial \xi}\right) = (\mu + \kappa)\left(\frac{\partial^2 u_y}{\partial x^2} + \frac{1}{l^2}\frac{\partial^2 u_y}{\partial \xi^2}\right) - \kappa\left(\frac{\partial v_m}{\partial x}\right) - \frac{1}{l}\frac{\partial p}{\partial \xi} \tag{3}$$

$$\rho j\left(u_x\frac{\partial v_m}{\partial x} + \frac{u_y}{l}\frac{\partial v_m}{\partial \xi}\right) = \gamma\left(\frac{\partial^2 v_m}{\partial x^2} + \frac{1}{l^2}\frac{\partial^2 v_m}{\partial \xi^2}\right) + \kappa\left(\frac{1}{l}\frac{\partial u_x}{\partial \xi} - \frac{\partial u_y}{\partial x}\right) - 2\kappa v_m \tag{4}$$

where $\xi = \frac{y}{l}$ is similarity variable, ρ, μ are the density and kinematic viscosity, j is the microinertia viscosity, κ, γ are the microrotation parameter and spin gradient viscosity respectively.

Neglecting the viscous dissipation, the equation for temperature field and concentration can be written as

$$\rho c_p\left(u_x\frac{\partial T}{\partial x} + \frac{u_y}{l}\frac{\partial T}{\partial \xi}\right) - \frac{\kappa_0}{c_p}\left(\frac{1}{l^2}\frac{\partial T}{\partial y^2}\right) = 0 \tag{5}$$

$$u_x\frac{\partial C}{\partial x} + \frac{u_y}{l}\frac{\partial C}{\partial \xi} - \left(\frac{D*}{l^2}\frac{\partial C}{\partial y^2}\right) = 0 \tag{6}$$

where T is the temperature, c_p is the specific heat at constant pressure, κ_0 is the thermal conductivity of fluid, C is the concentration of fluid particles, and $D*$ is the molecular diffusivity.

The boundary conditions for velocity, microrotation, temperature and concentration field can be written as

$$u_x = 0, u_y = v_1, v_m = -\frac{s}{l}\frac{\partial u}{\partial \xi} \quad \text{at } \xi = -1 \tag{7}$$

$$u_x = 0, u_y = v_2, v_m = \frac{s}{l}\frac{\partial u}{\partial \xi} \quad \text{at } \xi = 1$$

$$T = \begin{cases} T_1, & \xi = -1 \\ T_2, & \xi = 1 \end{cases} \tag{8}$$

$$C = \begin{cases} C_1, & \xi = -1 \\ C_2, & \xi = 1 \end{cases} \tag{9}$$

This complex system of nonlinear equations in Eqs. (1)-(4), Eq. (5) and Eq. (6) representing the present problem is solved after applying suitable transformations. The stream functions for velocity can be taken in the form [15]

$$\Phi(x, \xi) = \left(\frac{lU_0}{\alpha_0} - v_2 x\right) F(\xi) \tag{10}$$

where, $U_0 = \int_0^1 u_x(0, \xi) d\xi$ is the entrance velocity, and $\alpha_0 = 1 - \frac{v_1}{v_2}$.

Using the defined similarity transformations, the velocity, microrotation, temperature and concentration components are given by

$$\begin{aligned} u_x(x, \xi) &= \left(\frac{U_0}{\alpha_0} - \frac{v_2 x}{l}\right) f'(\xi), \quad u_y(x, \xi) = v_2 f(\xi), \\ v_m(x, \xi) &= \frac{1}{l}\left(\frac{U_0}{\alpha_0} - \frac{v_2 x}{l}\right) G(\xi) \\ \theta(\xi) &= \frac{T - T_1}{T_2 - T_1}, \qquad \phi(\xi) = \frac{C - C_1}{C_2 - C_1}. \end{aligned} \tag{11}$$

We see that this usual way of defined stream functions satisfies continuity equation and thus representing a valid fluid motion. Substituting Eq. (11) in Eqs. (1)-(4), Eq. (5) and Eq. (6), the dimensionless form of the governing equations can be obtained as

$$(1 + n_1) F'''' - n_1 G'' + S(F'F'' - FF''') - M^2 F'' = 0 \tag{12}$$

$$n_2 G'' - n_1 (F'' - 2G) - n_3 S(FG' - GF') = 0 \tag{13}$$

$$\theta'' + p_h (F'\theta - F\theta') = 0 \tag{14}$$

$$p'' + p_m (F'\phi - F\phi) = 0 \tag{15}$$

where $S = \frac{\rho v_2 h}{\mu}$ is the Reynolds number, $M^2 = \frac{\sigma_e h B_0^2}{\rho v_2}$ is the magnetic parameter, $Pr = \frac{\nu \rho c_p}{\kappa_0}$ is the Prandtl number with $p_h = SPr$, $S_c = \frac{\nu}{D*}$ is the Schmidt number with $p_m = S_c S$. Here, $n_1 = \frac{\kappa}{\mu}, n_2 = \frac{\gamma}{\mu h^2}, n_3 = \frac{j}{h^2}$ are the micropolar parameters respectively named vortex viscosity parameter, spin gradient viscosity parameter and microinertia density parameter.

The boundary conditions in Eq. (7), Eq. (8) and Eq. (9) takes the dimensionless form as

$$\begin{cases} \text{At } \xi = -1, & F = 1 - \alpha_0, & F' = G = 0, & \theta = \phi = 1 \\ \text{At } \xi = 1, & F = 1, & F' = G = 0, & \theta = \phi = 0 \end{cases} \tag{16}$$

We now have to solve the system of governing equations in Eqs. (12)-(15) subject to boundary conditions represented in Eq. (16) representing the fluid flow situation described.

3. Keller-Box Solution

Majority of the physical problems when modeled are finally derived into complex set of non-linear differential equations. It is well known that the exact analytical solutions to these governing equations are difficult to obtain. It is worthy to mention that the numerical techniques would give accurate, effective and efficient solutions. We use finite difference based numerical method popularly called as Keller-box method to solve the system of coupled non-linear equations for understanding the effects of various pertinent parameters of the flow. Because of its stability and efficiency, the box technique has been demonstrated in the literature to be a powerful tool for solving nonlinear differential equations. This method begins by introducing new variables into the governing system with boundary conditions, resulting in a set of first-order differential equations. The system of first-order equations is then discretized by substituting appropriate finite difference approximations. The non-linear algebraic equations are linearized using Newton's linearization method. A block tri-diagonal elimination scheme is then used to solve the resulting linear system. The detailed steps of this numerical procedure for the current problem are not presented here to save space. For all computations, a uniform step size of $\Delta\xi_i = 0.01$ is used, and the solutions are obtained with an error tolerance of 10^{-9}. The computational results for velocity profiles and microrotation are obtained for various sets of values of micropolar parameters n_1, n_2, and n_3, Reynolds number, and magnetic parameter.

4. Numerical Outcomes and Analysis

In this section, the numerical results obtained using Keller-box method is visualised using graphs and tables. The numerical finite difference-based method is yet again proved to be an efficient reliable technique to solve non-linear coupled governing equations. Figure 2 shows dimensionless velocity and microrotation profiles for fixed $M = 5$, $R = 1.5$, and $S = 10$, $\alpha_0 = 0.1$. These profiles are plotted for various micropolar parameters n_1, n_2 and n_3. The velocity profiles intersect at one point for $0 \leq \xi \leq 0.5$ for every combination of n_1, n_2 and n_3. Microrotation profile behaves differently for different micropolar parameters, whereas velocity profiles show the similar behaviour.

In Figure 3, profiles are displayed for various suction Reynolds number S with $n_1 = 0.1, n_2 = 0.01$ and $n_3 = 0.1, M = 5, \alpha_0 = 0.2$. Velocity profiles increase initially, achieving the minima for each curve, which shifts toward $\xi = 1.0$, and increases after that, with an increase in suction Reynolds number S. Microrotation profile rises with an increase in suction Reynolds number S, except the region near the plate.

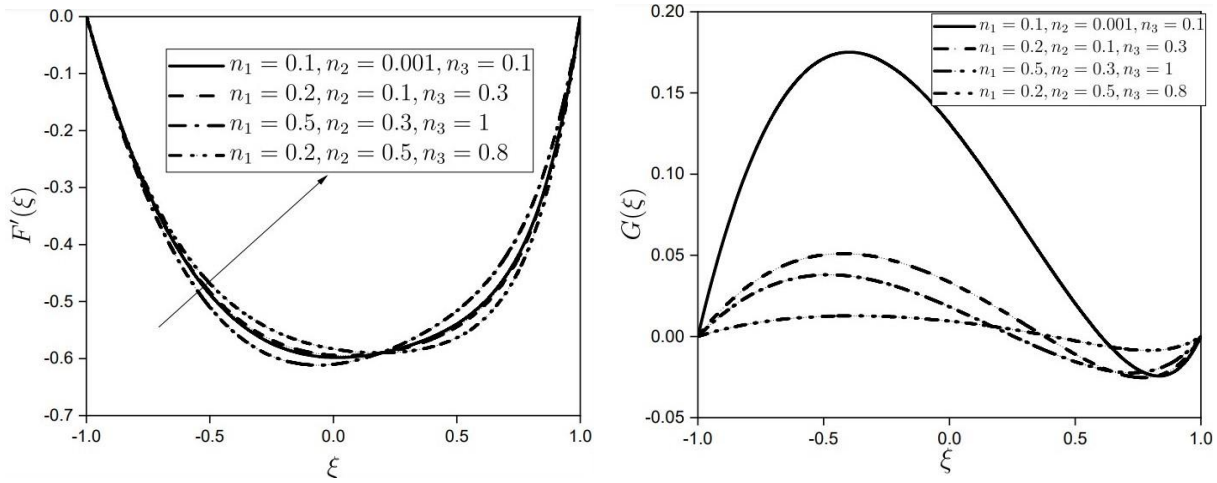

(a) (b)

Fig. 2. Dimensionless (a) Axial velocity, (b) Microrotation profile for various sets of parameters n_1, n_2 and n_3 with $M = 5$ and $R = 1.5, S = 10, \alpha_0 = 0.1$

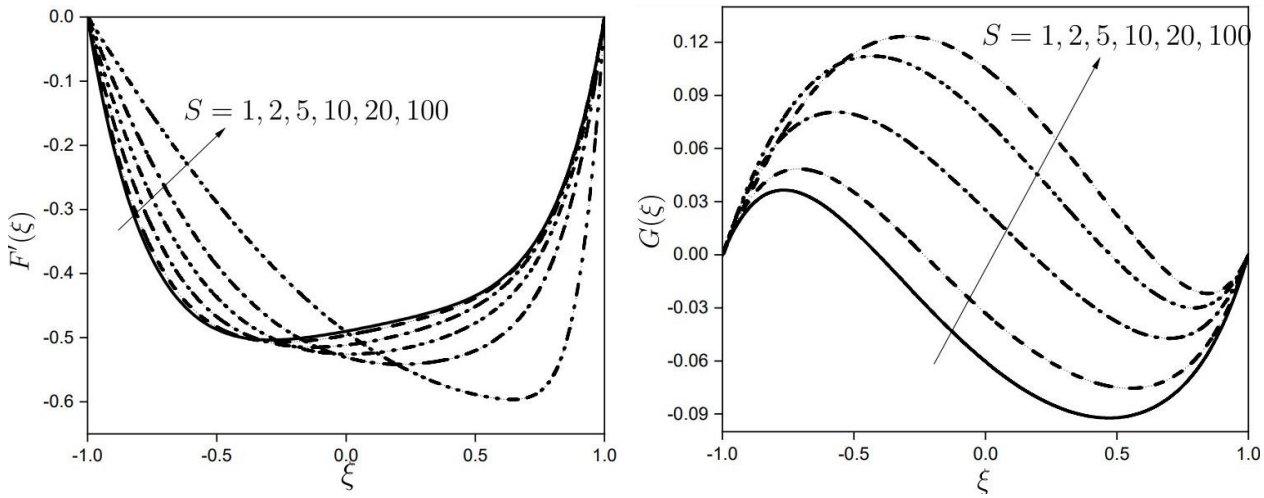

(a) (b)

Fig. 3. Dimensionless (a) Axial velocity, (b) Microrotation profile for various Reynolds number with $n_1 = 0.1, n_2 = 0.01$ and $n_3 = 0.1$, $M = 5, \alpha_0 = 0.2$

In Figure 4, profiles are plotted for various values of magnetic parameter M, with micropolar parameters $n_1 = 0.1, n_2 = 0.01$ and $n_3 = 0.1$, Suction Reynolds number $S = 5$, $\alpha_0 = 0.2$. Velocity profiles increase as the magnetic parameter M increases, but they become flatter. The effects of higher magnetic parameters tend to reduce the microrotation profiles curve at the upper and lower walls to zero. The outcome points out that an increment in the magnetic parameter enhances both velocity and microrotation profiles, although they tend to depress these profiles. The effect of the magnetic parameter M is to decrease microrotation at the upper and lower wall of the channel when $-0.8 < \xi < -0.3$ and $0.3 < \xi < 0.8$, respectively.

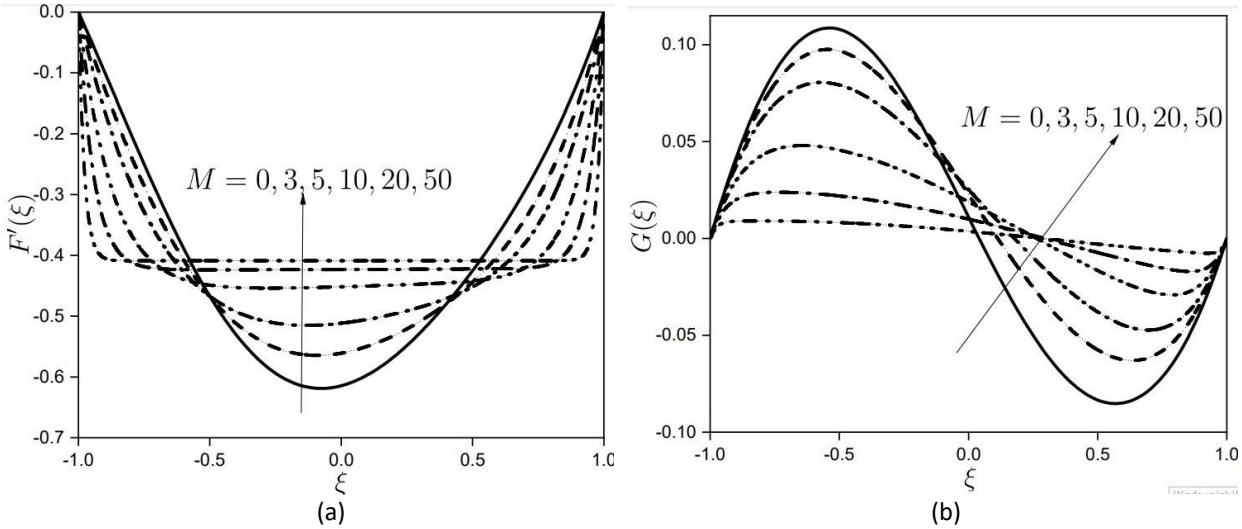

(a) (b)

Fig. 4. Dimensionless (a) Axial velocity, (b) Microrotation profile for various magnetic parameter with $n_1 = 0.1, n_2 = 0.01$ and $n_3 = 0.1, S = 5, \alpha_0 = 0.2$

In Figure 5, profiles are shown for different values of α_0 with micropolar parameters $n_1 = 0.1, n_2 = 0.01$ and $n_3 = 0.1$, suction Reynolds number $S = 5$, and magnetic parameter $M = 5$. Velocity profiles shows an increase with an increase in α_0 as it goes on depressing. In contrast, microrotation profiles decrease when ξ lies between -1.0 and 0.5, then increase after that, with an increase in α_0 till $\xi = 1.0$.

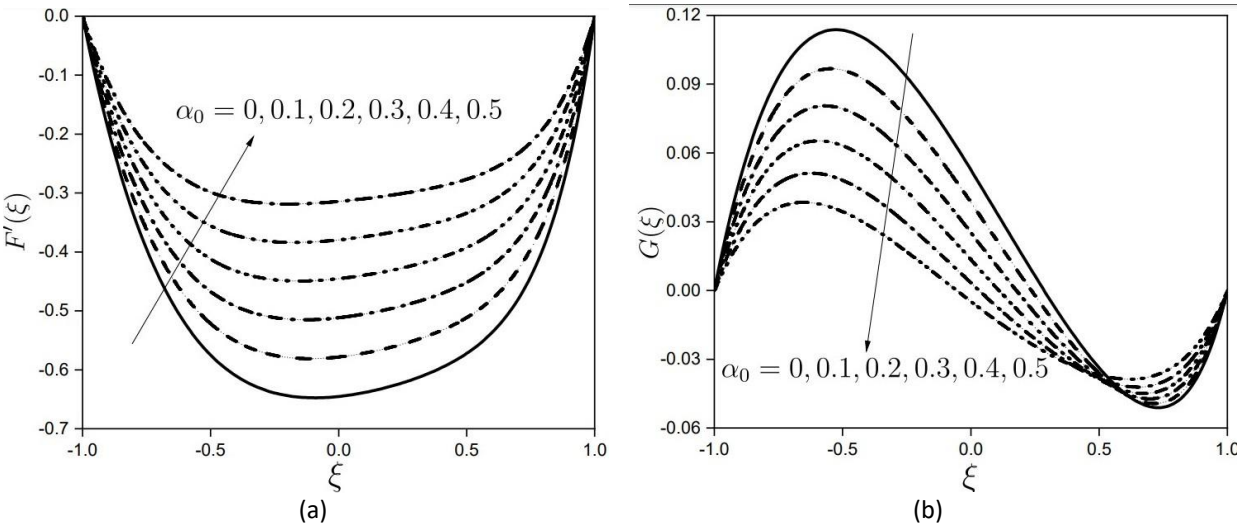

(a) (b)

Fig. 5. Dimensionless (a) Axial velocity, (b) Microrotation profile for various permiability parameter α_0 with $n_1 = 0.1, n_2 = 0.01$ and $n_3 = 0.1, S = 5, M = 5$

Micropolar parameters do alter the flow situation and the effects of these various micropolar parameters on the shear stress, heat, and mass transfer rates at both the boundary walls are tabulated in Table 1. It is witnessed in Table 2 that an increase in Reynolds number, considerably increases the shear stress while decreasing the heat and mass transfer rates.

Table 1
The shear stress, heat and mass transfer rates at both the boundary walls for various micropolar parameters

	$F''(-1)$	$F''(1)$	$\theta'(-1)$	$\theta'(1)$	$\phi'(-1)$	$\phi'(1)$
$n_1 = 0.1$, $n_2 = 0.001$, $n_3 = 0.1$	-1.50550911	2.968726603	-0.012017868	-0.256813696	-0.012407247	-0.362697983
$n_1 = 0.2$, $n_2 = 0.1$, $n_3 = 0.3$	-1.54885649	2.974085686	-0.01186139	-0.258342322	-0.012245699	-0.364856861
$n_1 = 0.5$, $n_2 = 0.3$, $n_3 = 1$	-1.55880485	2.570425489	-0.014944431	-0.236864391	-0.015428631	-0.334523579
$n_1 = 0.2$, $n_2 = 0.5$, $n_3 = 0.8$	-1.55770785	3.141786527	-0.010249973	-0.269667123	-0.010582072	-0.380850877

Table 2
The shear stress, heat and mass transfer rates at both the boundary walls for various Reynolds number

S	$F''(-1)$	$F''(1)$	$\theta'(-1)$	$\theta'(1)$	$\phi'(-1)$	$\phi'(1)$
1	-2.666203862	2.721072628	-0.028645114	-0.239593543	-0.029573216	-0.24824287
5	-1.996853075	2.794085138	-0.019811846	-0.245608924	-0.02045375	-0.254475406
10	-1.531290913	3.043451448	-0.011888394	-0.260731382	-0.012273578	-0.270143785
20	-1.128909404	3.674404706	-0.003570526	-0.294066579	-0.003686212	-0.304682382
50	-0.822755541	5.353601976	-0.00086254	-0.364669122	-0.000890486	-0.377833677

The effect of having different permeability at the two boundary walls on shear stress, heat, and mass transfer rates are depicted in Table 3. Table 4 demonstrates the outcome of varying Peclet number for heat and mass diffusion at both the boundary walls. It is observed that the effect of Peclet number is higher than others near the upper boundary, because of the presence of Prandtl number. Also, it is deduced that the concentration diffusion rate increases with the increase of Peclet number in top half of the channel.

Table 3
The shear stress, heat and mass transfer rates at both the boundary walls for various permeability parameter α_0

α_0	$F''(-1)$	$F''(1)$	$\theta'(-1)$	$\theta'(1)$	$\phi'(-1)$	$\phi'(1)$
0	-1.62437	3.454823	-0.00867	-0.25811	-0.00895	-0.26654
0.1	-1.53129	3.043451	-0.01189	-0.26073	-0.01228	-0.26924
0.2	-1.43175	2.64912	-0.02219	-0.26438	-0.02291	-0.273
0.3	-1.3238	2.271606	-0.02777	-0.26969	-0.02867	-0.27849
0.4	-1.20486	1.910436	-0.02062	-0.27658	-0.0213	-0.2856
0.5	-1.07166	1.564807	-0.01251	-0.28463	-0.01292	-0.29391

Table 4
The heat and mass transfer rates at both the boundary walls for diffetent Peclet numbers for heat p_h and mass diffusion p_m

p_h	$\theta'(-1)$	$\theta'(1)$	p_m	$\phi'(-1)$	$\phi'(1)$
0.1	-0.01189	-0.26073	0.1	-0.01228	-0.27269
0.2	-0.01387	-0.21886	0.2	-0.01433	-0.22889
0.3	-0.01417	-0.19606	0.3	-0.01464	-0.20506
0.4	-0.01386	-0.18078	0.4	-0.01431	-0.18907
0.5	-0.01852	-0.16945	0.5	-0.01913	-0.17722

5. Conclusions

In the present study, with the implementation of Keller-box method the equations governing heat and mass transfer analysis of micropolar fluid between porous channel of different permeability at the boundaries in the presence of external magnetic field is analysed. The numerical results showing effects of various micropolar parameters, Reynolds number, magnetic parameter, permeability variable on the flow were explained with the help of figures and tabulated data. It is important to note that the Reynolds number shows how important the inertia impact is in comparison to the viscous effect. Therefore, as Reynolds number rises, a decrease in velocity boundary layer thickness is observed. The external magnetic force plays an important role in controlling the fluid flow situation.

Acknowledgement
This research was not funded by any grant.

References
[1] Berman, Abraham S. "Laminar flow in channels with porous walls." *Journal of Applied physics* 24, no. 9 (1953): 1232-1235. https://doi.org/10.1063/1.1721476
[2] Sellars, John R. "Laminar flow in channels with porous walls at high suction Reynolds numbers." *Journal of Applied Physics* 26, no. 4 (1955): 489-490. https://doi.org/10.1063/1.1722024
[3] Yunan, S. W. "Further investigation of laminar flow in porous channels." *J. Appl. Phys* 27 (1956): 267-269. https://doi.org/10.1063/1.1722355
[4] Wah, Thein. "Laminar flow in a uniformly porous channel." *Aeronautical Quarterly* 15, no. 3 (1964): 299-310. https://doi.org/10.1017/S0001925900010908
[5] Robinson, W. A. "The existence of multiple solutions for the laminar flow in a uniformly porous channel with suction at both walls." *Journal of Engineering Mathematics* 10 (1976): 23-40. https://doi.org/10.1007/BF01535424
[6] Brady, J. F. "Flow development in a porous channel and tube." *The Physics of fluids* 27, no. 5 (1984): 1061-1067. https://doi.org/10.1063/1.864735
[7] Cox, Stephen M. "Analysis of steady flow in a channel with one porous wall, or with accelerating walls." *SIAM Journal on Applied Mathematics* 51, no. 2 (1991): 429-438. https://doi.org/10.1137/0151021
[8] King, J. R., and S. M. Cox. "Asymptotic analysis of the steady-state and time-dependent Berman problem." *Journal of engineering mathematics* 39, no. 1 (2001): 87-130. https://doi.org/10.1007/978-94-010-0698-9_7
[9] Eringen, A. Cemal. "Theory of micropolar fluids." *Journal of mathematics and Mechanics* (1966): 1-18. https://doi.org/10.1512/iumj.1967.16.16001
[10] Eringen, A. Cemal. "Theory of anisotropic micropolar fluids." *International Journal of Engineering Science* 18, no. 1 (1980): 5-17. https://doi.org/10.1016/0020-7225(80)90003-8
[11] Ariman, T. M. A. N. D., M. A. Turk, and N. D. Sylvester. "Microcontinuum fluid mechanics—a review." *International Journal of Engineering Science* 11, no. 8 (1973): 905-930. https://doi.org/10.1016/0020-7225(73)90038-4
[12] Ariman, T. T. N. D., M. A. Turk, and N. D. Sylvester. "Applications of microcontinuum fluid mechanics." *International Journal of Engineering Science* 12, no. 4 (1974): 273-293. https://doi.org/10.1016/0020-7225(74)90059-7
[13] Lukaszewicz, G. "Micropolar fluids. Theory and applications. Modeling and Simulation in Science, Engineering and Technology, Birkhuser Boston." *Inc., Boston, MA* (1999). https://doi.org/10.1007/978-1-4612-0641-5_5
[14] Sastry, V. U. K., and V. Rama Mohan Rao. "Numerical solution of micropolar fluid flow in a channel with porous walls." *International Journal of Engineering Science* 20, no. 5 (1982): 631-642. https://doi.org/10.1016/0020-7225(82)90117-3
[15] Na, T-Y., and I. Pop. "Boundary-layer flow of a micropolar fluid due to a stretching wall." *Archive of Applied Mechanics* 67 (1997): 229-236. https://doi.org/10.1007/s004190050113
[16] Desseaux, A., and Neil Kelson. "Solutions for the flow of a micropolar fluid in a porous channel." In *Proceedings of the 4th Biennial Engineering Mathematics and Application Conference*, pp. 115-118. Engineering Mathematics Group of ANZIAM, 2000.
[17] Bhat, Ashwini, and Nagaraj N. Katagi. "Micropolar fluid flow between a non-porous disk and a porous disk with slip: Keller-box solution." *Ain Shams Engineering Journal* 11, no. 1 (2020): 149-159. https://doi.org/10.1016/j.asej.2019.07.006

[18] Kelson, N. A., and T. W. Farrell. "Micropolar flow over a porous stretching sheet with strong suction or injection." *International Communications in Heat and Mass Transfer* 28, no. 4 (2001): 479-488. https://doi.org/10.21914/anziamj.v44i0.692

[19] Joneidi, A. A., D. D. Ganji, and M. Babaelahi. "Micropolar flow in a porous channel with high mass transfer." *International Communications in Heat and Mass Transfer* 36, no. 10 (2009): 1082-1088. https://doi.org/10.1016/j.icheatmasstransfer.2009.06.021

[20] Keller, Herbert B. "Some computational problems in boundary-layer flows." In *Proceedings of the Fourth International Conference on Numerical Methods in Fluid Dynamics: June 24–28, 1974, University of Colorado*, pp. 1-21. Berlin, Heidelberg: Springer Berlin Heidelberg, 2005.

[21] Keller, Herbert B. "Numerical methods in boundary-layer theory." *Annual Review of Fluid Mechanics* 10, no. 1 (1978): 417-433. https://doi.org/10.1146/annurev.fl.10.010178.002221

[22] Vajravelu, Kuppalapalle, and Kerehalli V. Prasad. "Keller-box method and its application." In *Keller-Box Method and Its Application*. De Gruyter, 2014. https://doi.org/10.1515/9783110271782

[23] Bhat, Ashwini, Nagaraj N. Katagi, and N. M. Bujurke. "Analysis of Laminar Flow in a Porous Pipe with Slip Velocity." *Journal of Mechanical Engineering Research and Developments* 40, no. 4 (2017): 1-11.

[24] Adnan, Nurul Shahirah Mohd, Norihan Md Arifin, Norfifah Bachok, and Fadzilah Md Ali. "Stability analysis of MHD flow and heat transfer passing a permeable exponentially shrinking sheet with partial slip and thermal radiation." *CFD Letters* 11, no. 12 (2019): 34-42.

[25] Wahid, Nur Syahirah, Mohd Ezad Hafidz Hafidzuddin, Norihan Md Arifin, Mustafa Turkyilmazoglu, and Nor Aliza Abd Rahmin. "Magnetohydrodynamic (MHD) slip darcy flow of viscoelastic fluid over a stretching sheet and heat transfer with thermal radiation and viscous dissipation." *CFD Letters* 12, no. 1 (2020): 1-12.

[26] Bhat, Ashwini, and Nagaraj N. Katagi. "Influence of Slip Velocity on Micropolar Fluid Through a Porous Channel: Using Keller-Box Method." *Journal of Advanced Research in Fluid Mechanics and Thermal Sciences* 66, no. 2 (2020): 49-64.